Solar Energy Materials & Solar Cells 152 (2016) 111–117

Contents lists available at ScienceDirect

Solar Energy Materials & Solar Cells

journal homepage: www.elsevier.com/locate/solmat

Two-dimensional modeling of TiO_2 nanowire based organic–inorganic hybrid perovskite solar cells

Xiaojie Wu [a], Ping Liu [b], Li Ma [a], Qian Zhou [a], Yongsheng Chen [a,*], Jingxiao Lu [a], Shi-e Yang [a]

[a] Key Lab of Material Physics, Department of Physics, Zhengzhou University, Zhengzhou 450052, PR China
[b] School of Electric and Information Engineering, Zhongyuan University of Technology, Zhengzhou 450007, PR China

ARTICLE INFO

Article history:
Received 16 November 2015
Received in revised form
18 March 2016
Accepted 20 March 2016
Available online 12 April 2016

Keywords:
Perovskite
Mesoscopic solar cells
Device simulation
TiO_2 nanowire array

ABSTRACT

Organo-metal halide perovskite solar cells have shown unique charms in the upgrade rate of maximum power conversion efficiency, the diversity of device architecture and facilitated fabrication process. And the clear understanding of the role of each component and the basic working mechanisms in solar cells is important for further improvement in efficiency, especially for mesoscopic perovskite solar cells. Here, a two-dimensional modeling of the TiO_2 nanowire-based organic–inorganic hybrid perovskite solar cells was performed combining the optical and electrical responses to reveal the impact of the properties of TiO_2 nanowire array and absorber layer. Simulation results show a great dependence of device performance on the electron concentration of TiO_2 nanowires, which decided the electron field distribution inside cells, and an optimum thickness of 600 nm is obtained for the TiO_2 nanowires with low electron concentration. The collection of carriers is primarily within perovskite itself, and the ratio through TiO_2 nanowire is less than 5%. These findings can facilitate device optimization and enhance the performance of the perovskite solar cells.

1. Introduction

Organic–inorganic halide perovskite solar cells (PSCs) have attracted considerable attention in the last few years due to the breaking of the stubborn trade-off between power conversion efficiency and fabrication cost [1,2], where the reported efficiencies have doubled up from the about 10% [3,4] in 2012 to current certified 22.1% (http://www.nrel.gov/ncpv/images/efficiency_chart.jpg), based on the improvements of fabrication technologies, device architecture, morphology and crystallinity of the perovskite films [5–9]. In these progresses, one of the most intriguing charms surprised researchers is that high efficiencies of over 15% are retrieved obtained using the mesoporous scaffold structure and planar junction configuration, respectively, indicating that the former structure stemmed from the dye-sensitized solar cells is not a requirement to achieve the enhanced performances. Moreover, the presence of mesoporous scaffold obviously constrains the perovskite grain size to nanoscale [10] and the degree of crystallization to about 30% [11]. However, some clear advantages of PSCs based on TiO_2 nanostructure have been observed. For example, the hysteresis issue for planar devices can be effectively minimized by the use of mesoporous TiO_2 scaffold [12–14]. Moreover, the carrier-collection efficiencies are enhanced, especially for the systems where the carrier diffusion length is much shorter than the photon absorption length [15]. Besides, the performance of solar cells is boosted by placing a compact perovskite overlayer on top of the $CH_3NH_3PbI_3/TiO_2$ nanocomposite, and a 200 nm thick TiO_2 scaffold is optimized [16,17], in which the performance of device is primarily ruled by the overlayer, and the main role of scaffold is believed to help modify the electron selective contact and promote an effect regarding electrical field distribution in the perovskite growth process [10]. On the other hand, cells fabricated without a mesoporous metal oxides layer, or in the presence of Al_2O_3 instead of TiO_2, showed to be much less stable, even in the dark [2]. Thus, for future higher performance of PSCs with 22–25% efficiencies, whether the mesoporous TiO_2 scaffold layer is required or to what extent remains an intriguing unknown.

To reveal the role of TiO_2 scaffold layer in PSCs, Moser et al. [3,18] overcame the challenges of a spectral overlap encountered in the earlier study and presented clear evidence of efficient electron injection from $CH_3NH_3PbI_3$ into TiO_2. Marchioro et al. [18] showed that the amount of long-lived charges in the $TiO_2/CH_3NH_3PbI_3$/HTM (hole transport material) devices is higher than that in the $Al_2O_3/CH_3NH_3PbI_3$/HTM devices by using transient absorption spectroscopy, suggesting that the use of TiO_2 as the electron acceptor and transporter is advantageous. Nevertheless, Snaith et al. [4] showed that the charge collection in the Al_2O_3-based PSCs is faster than the

* Corresponding author. Tel.: +86 371 677 66917.
E-mail address: chysh2003@zzu.edu.cn (Y. Chen).

http://dx.doi.org/10.1016/j.solmat.2016.03.017
0927-0248/

TiO_2-based devices by using transient photocurrent measurements, indicating that perovskite itself is more efficient in carrier transport than mesoporous TiO_2. Furthermore, in the continuous excitation regime, spiro-OMeTAD (2,2′,7,70-tetrakis(N,N-p-dimethoxy-phenylamino)-9,90-spirobifl-uorene) extracts the holes more efficiently in Al_2O_3 than in TiO_2-based samples [10]. So, the judicious working mechanisms of PSCs based on mesoporous TiO_2 scaffold layer has yet to be fully established.

Device simulation can aid in elucidating the relationship between material property and device performance. PSCs based on planar architecture thus far have been successfully modeled using one-dimensional device simulators [19–21]. In our previous study [22,23], we analyzed the working principles of planar PSCs using a two-dimensional (2D) modeling carried out on COMSOL Multiphysics. Anaya et al. [24] described both theoretically and experimentally the optical response of mesostructured PSCs. But, to the best of our knowledge, a completely simulation of mesoscopic solar cells, including the optical and transport properties, has not been investigated. In this study, to understand the operation mechanism and optimum design of the device, we performed 2D simulations of TiO_2 nanowire-based PSCs which link both optical absorption and carrier transport by COMSOL Multiphysics.

2. Device simulation parameters

The schematic of the TiO_2 nanowire-based organic–inorganic hybrid PSC is shown in Fig. 1. The cell was constructed on a fluorine-doped tin oxide (FTO, 500 nm)-coated glass, serving as the transparent electrode and substrate. A compact TiO_2 thin film was used as electron transport material (ETM). An array of TiO_2 nanowires with a radius of 10 nm or 20 nm, which served as scaffold layer, was laterally arranged over the compact TiO_2 layer attained a porosity of 50%, followed by the infiltration of the $CH_3NH_3PbI_3$ perovskite material. Spiro-OMeTAD was further employed as HTM layer, and Au film (100 nm) was cathode.

A modular two-steps 2D simulation [22,23] was carried out on COMSOL Multiphysics. The first step was to perform an exact full field electromagnetic calculation based on 2D Maxwell's equations in the frequency domain. The standard AM 1.5G spectrum was introduced as the incident light source, and the n, k values of the stacks, that are, FTO, TiO_2, $CH_3NH_3PbI_3$, spiro-OMeTAD, and Au, were taken from literatures [25–27], as shown in Fig. S1. Furthermore, the photo-generated rate extracted from the optical calculation was used for the exact electrical characteristics calculations, in which only four layers, namely n-type compact TiO_2, n-type TiO_2 nanowires, low p-type doped $CH_3NH_3PbI_3$ and n-type

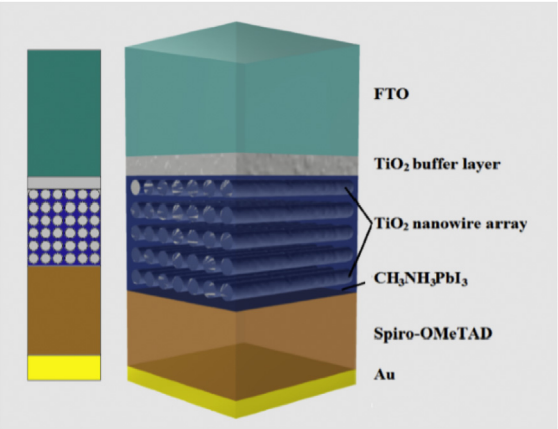

Fig. 1. The two (a) and three (b) -dimensional cross-sectional schematics of the TiO_2 nanowire-based PSC.

Table 1
Input parameters of device simulation.

Parameters	Compact TiO_2	TiO_2 nanowire	$CH_3NH_3PbI_3$	Spiro-OMeTAD
Thickness (nm)	50	300 (variable)	300 (variable)	350
Radius (nm)	...	10 or 20	...	...
N_A (cm^{-3})	...	...	10^{13} [19]	10^{18} [34]
N_D (cm^{-3})	10^{19} [32]	10^{16} (variable)	...	...
N_C/N_V (cm^{-3})	$10^{19}/10^{19}$	$10^{19}/10^{19}$	2.2×10^{18}/ 1.8×10^{19} [19]	$10^{20}/10^{20}$
ε_r	9.0 [19]	9.0	6.5 [36]	3.0 [35]
χ (eV)	4.0	4.0	3.93 [3]	2.45 (variable)
E_g (eV)	3.2	3.2	1.5 [3]	3.0
μ_n/μ_p (cm^2/V s)	0.02/2 [33]	0.02/2	0.5/0.5 [28]	2/0.01 [13]
τ_n/τ_p (ns)	5/2	5/2	8/8 (variable)	0.1/0.1

spiro-OMeTAD, were considered. The input parameters were summarized in Table 1 for each layer. Here, N_A and N_D denote acceptor and donor densities, ε_r is relative permittivity, χ is electron affinity, E_g is bandgap energy, N_C and N_V are effective state density of conduction and valence bands, μ_n and μ_p are mobilities of electron and hole. τ_n and τ_p are the life times of electron and hole for trap-assisted recombination, and are set to be identical for $CH_3NH_3PbI_3$, which is consistent with ambipolar characteristics of the carriers [28,29]. The values of electron diffusion coefficient, D_n, and electron diffusion length, L_n, for $CH_3NH_3PbI_3$, calculated to be same [30], are closely related to the distribution of electrical field in film [10] and the grain size [31]. So, we assumed $\tau_n=\tau_p=8$ ns to obtain carrier diffusion length of 100 nm ($L_n=(D_n\tau_n)^{1/2}$, $D_n=0.013$ cm^2 s^{-1}), which is a similar value to the literature [28]. In the interfaces between compact TiO_2, TiO_2 nanowires, $CH_3NH_3PbI_3$ and spiro-OMeTAD, the carrier recombination is neglected. Ideal Ohmic and Schottky contacts with surface recombination speed of 1×10^7 cm/s for front and back contacts were used respectively. The quantum confinement effects within the PSCs were not considered in this simulation. Finally, information on performance, including short-circuit current density (J_{SC}), J–V curve, open-circuit voltage (V_{OC}), fill factor (FF), conversion efficiency (η), *etc.* can all be obtained for the optimization of PSCs designs.

3. Results and discussion

In the optical modeling process, the spatial distribution of the electric field in the multilayer stack was calculated. Fig. S2 depicts the calculated distribution of electric field inside PSC comprising a 300 nm thick TiO_2 nanowires array with a nanowire radius of 10 nm under different wavelength irradiation. The distribution of electric field inside PSCs presents a streaks characteristic, and the introduction of TiO_2 nanowires array almost has not any turbulence on the optical field in $CH_3NH_3PbI_3$ due to the smaller radius compared to incident light wavelength. With the increase of wavelength, the field intensities in FTO and compact TiO_2 layers are increased, and the penetration depth of the electric field in PSCs is enhanced. The absorption spectra of each constituent of the PSCs can be deduced from the calculated spatial distribution of the electric field intensity inside the PSCs, and the result is shown in Fig. 2. Note that the effect of glass substrate on the optical properties is not considered in this simulation. The total absorbance is lower than 1 due to the optical losses of reflectance and transmittance. At wavelength of 300 nm, the incident light is mainly absorbed by the FTO and TiO_2 (compact TiO_2 and TiO_2 nanowires) layers. With increasing of wavelength the